Jacqueline E. Noll, Duncan R. Hewett, Sharon A. Williams, Kate Vandyke, Chung Kok, Luen B. To, and Andrew C.W. Zannettino

SAMSN1 is a tumor suppressor gene in multiple myeloma

Neoplasia, 2014; 16(7):572-585

Originally published at:
http://doi.org/10.1016/j.neo.2014.07.002

NEOPLASIA
www.neoplasia.com

Volume 16 Number 7 July 2014 pp. 572–585 572

SAMSN1 Is a Tumor Suppressor Gene in Multiple Myeloma[1,2]

Jacqueline E. Noll[*,†,3], Duncan R. Hewett[*,†,3], Sharon A. Williams[*,†,3], Kate Vandyke[*,†], Chung Kok[‡], Luen B. To[†] and Andrew C.W. Zannettino[*,†]

*Myeloma Research Laboratory, School of Medical Sciences, Faculty of Health Science, University of Adelaide, Adelaide, Australia; [†]Department of Haematology, Centre for Cancer Biology, SA Pathology, Adelaide, Australia; [‡]Acute Myeloid Leukaemia Laboratory, Department of Haematology, Centre for Cancer Biology, SA Pathology, Adelaide, Australia

Abstract

Multiple myeloma (MM), a hematological malignancy characterized by the clonal growth of malignant plasma cells (PCs) in the bone marrow, is preceded by the benign asymptomatic condition, monoclonal gammopathy of undetermined significance (MGUS). Several genetic abnormalities have been identified as critical for the development of MM; however, a number of these abnormalities are also found in patients with MGUS, indicating that there are other, as yet unidentified, factors that contribute to the onset of MM disease. In this study, we identify a *Samsn1* gene deletion in the 5TGM1/C57BL/KaLwRij murine model of myeloma. In addition, *SAMSN1* expression is reduced in the malignant CD138+ PCs of patients with MM and this reduced expression correlates to total PC burden. We identify promoter methylation as a potential mechanism through which *SAMSN1* expression is modulated in human myeloma cell lines. Notably, re-expression of Samsn1 in the 5TGM1 murine PC line resulted in complete inhibition of MM disease development *in vivo* and decreased proliferation in stromal cell–PC co-cultures *in vitro*. This is the first study to identify deletion of a key gene in the C57BL/KaLwRij mice that also displays reduced gene expression in patients with MM and is therefore likely to play an integral role in MM disease development.

Neoplasia (2014) 16, 572–585

Introduction

Multiple myeloma (MM) is an incurable hematological malignancy characterized by the clonal proliferation of malignant plasma cells (PCs) within the bone marrow (BM). MM is the second most common hematological malignancy after non-Hodgkin's lymphoma, with approximately 20,000 newly diagnosed patients each year in the USA [1]. The main clinical manifestations of MM are the development of osteolytic bone lesions, bone pain, hypercalcemia, renal insufficiency, suppressed immunoglobulin production, and increased BM angiogenesis. Despite recent advances in treatment, MM remains almost universally fatal with a 10-year survival rate of approximately 17% [2].

MM encompasses a range of clinical variants ranging from monoclonal gammopathy of undetermined significance (MGUS) and smoldering/indolent MM to more aggressive disseminated forms of MM and PC leukemia. It is now widely accepted that most, if not all, MMs are preceded by a premalignant MGUS [3]. MGUS is defined as a benign proliferation of PCs and is clinically characterized by the presence of monoclonal protein (or "paraprotein") of <3 g/dl, clonal PCs constituting <10% of the BM, and the absence of organ damage [4]. Patients with MGUS have a risk of developing overt MM

Address all correspondence to: Andrew Zannettino, PhD, Discipline of Physiology, School of Medical Sciences, Faculty of Health Science, University of Adelaide, Adelaide, Australia and Bone and Cancer Laboratories, Level 3, Department of Haematology, SA Pathology, Frome Road, Adelaide 5000, South Australia, Australia. E-mail: andrew.zannettino@adelaide.edu.au

[1] This article refers to supplementary materials, which are designated by Table S1 and Figures S1 and S2 and are available online at www.neoplasia.com.

[2] J.E.N. is supported by the Veronika Sacco Clinical Cancer Research Fellowship from the Florey Medical Research Foundation, University of Adelaide. D.R.H. is supported by the Cancer Australia/Leukemia Foundation Priority-Driven Collaborative Cancer Research Scheme, Project 1030518. The authors report no conflicts of interest.

[3] These authors contributed equally to this work.

Received 29 May 2014; Revised 1 July 2014; Accepted 3 July 2014

1476-5586/14
http://dx.doi.org/10.1016/j.neo.2014.07.002

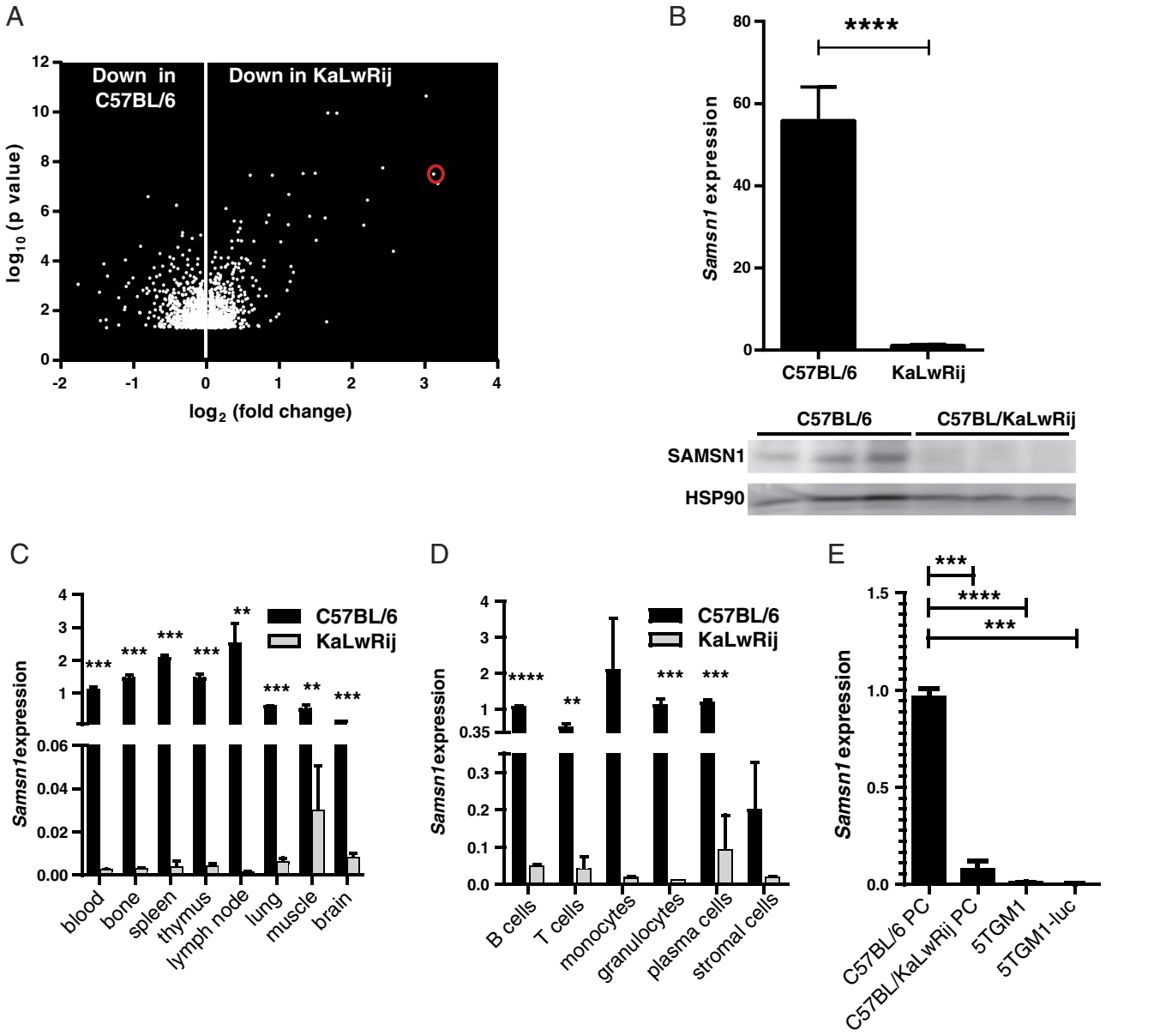

Figure 1. Global loss of *Samsn1* expression is a feature of the 5TGM/C57BL/KaLwRij mouse model of myeloma. (A) The gene expression profiles of the long bones of C57BL/6 ($n = 4$) and C57BL/KaLwRij ($n = 4$) mice were compared using the Illumina Mouse WG-6 v2.0 BeadChip. Fold change in gene expression between the strains is plotted against the significance of the change. Each data point represents one gene. *Samsn1* is circled. (B) The reduced expression of *Samsn1* in C57BL/KaLwRij bones was confirmed in independent samples by real-time PCR ($n = 4$ per group) and Western blot. ****$P < .0001$, *t* test. (C) RNA was isolated from C57BL/KaLwRij ($n = 3$) and C57BL/6 ($n = 3$) derived tissues and *Samsn1* mRNA expression was assessed by real-time PCR. (D) Cells were isolated from C57BL/KaLwRij ($n = 3$) and C57BL/6 ($n = 3$) BM (PCs and stromal cells) and peripheral blood (other cell subsets). *Samsn1* mRNA expression was assessed by real-time PCR. (E) 5TGM1 cells express negligible *Samsn1*, as determined by real-time PCR. C57BL/KaLwRij and C57BL/6 mouse PCs are shown for comparison. ****$P < .0001$; ***$P < .001$; **$P < .01$; *t* test.

at a rate of 1% per year; however, the time to progression varies greatly between patients [5].

Patients with MM can be stratified into various subgroups based on the presence of defined genetic abnormalities in their malignant PCs [6]. These genetic abnormalities include, but are not limited to, del(13) [7], del(16q) [8], del(17p) [9], gain of 1q21 [10], as well as translocations involving the immunoglobulin heavy chain locus, i.e., t(4;14)(p16.3;q32) and t(14:16)(q32;q23) [11,12], all of which are associated with poor prognosis. While these abnormalities are believed to play a major causative role in disease development, studies suggest that many of them are already present in the clonal PCs of patients with MGUS [13,14]. Therefore, it is likely that additional, as yet undefined, factors are required for the progression from asymptomatic MGUS to overt malignant MM. To this end, recent studies suggest that changes in gene expression, including up-regulation and/or down-regulation of key genes, which occurs through epigenetic mechanisms, may play a key role in the development of symptomatic MM [15].

Table 1. Genes Differentially Expressed in the Long Bones of C57BL/KaLwRij and C57BL/6 Mice

Symbol	Definition	Fold change	Direction
Gbp1	*Guanylate binding protein 1*	4.450412306	Increase
Ddit4	*DNA damage–inducible transcript 4*	4.240428329	Increase
Hist4h4	*Histone cluster 4, H4*	3.37437661	Increase
Tmod4	*Tropomodulin 4*	3.353338216	Increase
Angptl7	*Angiopoietin-like 7*	3.283043806	Increase
Mx2	*Myxovirus (influenza virus) resistance 2*	3.249176241	Increase
Lyplal1	*Lysophospholipase-like 1*	3.139500408	Increase
Ifit3	*Interferon-induced protein with tetratricopeptide repeats 3*	3.030790225	Increase
Pttg1	*Pituitary tumor–transforming 1*	2.94256646	Increase
Oas2	*2′-5′ oligoadenylate synthetase 2*	2.731815404	Increase
Oas1g	*2′-5′ oligoadenylate synthetase 1G*	2.704346478	Increase
Usp18	*Ubiquitin specific peptidase 18*	2.538251457	Increase
Ifi27l2a	*Interferon, alpha-inducible protein 27*	2.533970976	Increase
Gbp7	*Guanylate binding protein 7*	2.508261909	Increase
Pisd-ps3	*Phosphatidylserine decarboxylase, pseudogene 3*	2.436705673	Increase
Per1	*Period homolog 1 (Drosophila)*	2.397020089	Increase
Sct	*Secretin*	2.384120243	Increase
Irf7	*Interferon regulatory factor 7*	2.378730781	Increase
Pdk4	*Pyruvate dehydrogenase kinase, isoenzyme 4*	2.346674916	Increase
Rtp4	*Receptor transporter protein 4*	2.337282308	Increase
Oasl2	*2′-5′ oligoadenylate synthetase-like 2*	2.242105245	Increase
Msc	*Musculin*	2.210238416	Increase
Hist1h4b	*Histone cluster 1, H4b*	2.207251464	Increase
Igh-VJ558	*PREDICTED: immunoglobulin heavy chain (J558 family)*	2.193584071	Increase
Rbp7	*Retinol binding protein 7, cellular*	2.191502007	Increase
Pydc4	*Pyrin domain containing 4*	2.187228581	Increase
Npy	*Neuropeptide Y*	2.170017985	Increase
Erdr1	*Erythroid differentiation regulator 1*	2.158546243	Increase
Thsd4	*Thrombospondin, type I, domain containing 4, transcript variant 1*	2.133757168	Increase
Bfsp2	*Beaded filament structural protein 2, phakinin*	2.110095069	Increase
Paip1	*Polyadenylate binding protein-interacting protein 1, transcript variant 1*	2.098810627	Increase
Cyr61	*Cysteine rich protein 61*	2.036144571	Increase
Mgst1	*Microsomal glutathione S-transferase 1*	57.60499461	Decrease
Samsn1	*SAM domain, SH3 domain and nuclear localization signals, 1*	51.76062024	Decrease
Entpd4	*Ectonucleoside triphosphate diphosphohydrolase 4*	19.42186718	Decrease
Slc25a37	*Solute carrier family 25, member 37*	16.9916612	Decrease
Slc22a4	*Solute carrier family 22 (organic cation transporter), member 4*	14.15791584	Decrease
H2afj	*H2A histone family, member J*	11.74400026	Decrease
Sparc	*Secreted acidic cysteine rich glycoprotein*	9.001990237	Decrease
Bbs4	*Bardet-Biedl syndrome 4 (human)*	3.525644472	Decrease
Kif3a	*Kinesin family member 3A*	3.134149503	Decrease
Tipin	*Timeless interacting protein*	2.959086767	Decrease
Cdkn1b	*Cyclin-dependent kinase inhibitor 1B*	2.908346173	Decrease
Vsig4	*V-set and immunoglobulin domain containing 4*	2.825793418	Decrease
Hist1h3f	*Histone cluster 1, H3f*	2.804314199	Decrease
Sfrp4	*Secreted frizzled-related protein 4*	2.725447254	Decrease
Rps3a	*Ribosomal protein S3a*	2.493150544	Decrease
Pml	*Promyelocytic leukemia (Pml), transcript variant 1*	2.333694965	Decrease
Hist1h4i	*Histone cluster 1, H4i*	2.240988119	Decrease
Dcp1b	*DCP1 decapping enzyme homolog b (S. cerevisiae)*	2.233498058	Decrease
Aoah	*Acyloxyacyl hydrolase*	2.202379368	Decrease
Adpgk	*ADP-dependent glucokinase*	2.172734661	Decrease
Trim2	*Tripartite motif protein 2*	2.151279536	Decrease
Hdgf	*Hepatoma-derived growth factor*	2.128178262	Decrease
Hist1h4f	*Histone cluster 1, H4f*	2.085821933	Decrease
Plac9	*Placenta specific 9*	2.038744521	Decrease
Tbc1d9b	*TBC1 domain family, member 9B*	2.012406842	Decrease
Arhgap26	*Rho GTPase activating protein 26*	2.005116414	Decrease

Expression in C57BL/KaLwRij bone relative to expression in C57BL/6 bone.

In the present study, we used gene expression arrays to identify transcriptomic differences between the closely related C57BL/KaLwRij and C57BL/6 mouse strains that could account for the age-dependent predisposition of C57BL/KaLwRij mice to develop a MM-like disease [16,17]. From these analyses, Samsn1 was identified as one of the most significantly downregulated genes in the C57BL/KaLwRij mouse strain. Further analysis revealed that the loss of Samsn1 expression was due to a homozygous gene deletion encompassing the entire *Samsn1* coding region in the C57BL/KaLwRij mouse.

SAMSN1 (also known as HACS1, SLY2, and SASH2) encodes a member of the SLY family of cytoplasmic adaptor proteins and is predominantly expressed in the hematopoietic compartment, with lower levels of expression in heart, brain, placenta, and lung [18]. Studies in *Samsn1* knockout mice, which are viable and fertile, indicate that it may act to moderate adaptive immune responses [19]. *Samsn1* has also been shown to play a role in B cell activation and differentiation [20] and has been implicated as a tumor suppressor gene in lung cancer [21]. However, to date, the precise cellular role of SAMSN1 remains poorly understood.

In this study, we also show that *SAMSN1* expression is low or absent in a proportion of human myeloma cell lines (HMCLs) and MM patient–derived PCs compared to PCs isolated from patients with MGUS and healthy controls. Furthermore, we show that methylation of the *SAMSN1* promoter is a likely mechanism of reduced *SAMSN1* expression in human MM cells. Importantly, overexpression of Samsn1 in the murine MM cell line, 5TGM1, completely inhibited MM disease development *in vivo* and reduced proliferation in stromal cell–PC co-cultures *in vitro*, suggesting that SAMSN1 may function as a tumor suppressor in MM.

Materials and Methods

Gene Expression Profiling by Microarray

Femora and tibiae from age- and sex-matched C57BL/6 and C57BL/KaLwRij mice were extracted, cleaned thoroughly, and snap-frozen in liquid nitrogen. Frozen bones were pulverized under liquid nitrogen in a mortar and pestle, and RNA was extracted using the high salt method [22]. Briefly, bone powder was homogenized in 4 M guanidinium thiocyanate containing 0.5% sarcosyl and 4.5 mM 2-mercaptoethanol by drawing repeatedly through a 19 G needle. Debris was removed by centrifugation and RNA was separated from proteins and DNA using acidified phenol/chloroform. Salt was removed by isopropanol precipitation and washing with 70% ethanol. The extracted RNA was further purified using a silica gel-based membrane column (Qiagen RNeasy kit; Qiagen, Valencia, CA). RNA was submitted to the Australian Genome Research Facility (Parkville, Australia) for labeling and array hybridization to the Illumina Mouse WG-6 v2.0 BeadChip. Data analysis was performed at the Australian Genome Research Facility. Four biologic replicates of each mouse strain were analyzed.

Real-Time Polymerase Chain Reaction

Total RNA was isolated using TRIzol reagent (Life Technologies, Carlsbad, CA) unless otherwise specified. RNA was reverse transcribed using Superscript III (Life Technologies) or Sensiscript (Qiagen) as per the manufacturers' instructions. Real-time polymerase chain reaction (PCR) was conducted on a Rotor-Gene 3000 (Corbett Research, Mortlake, Australia) using the following primers: mouse/human *Actb* (F: 5′-TTGCTGACAG-GATGCAGAAG-3′ and R: 5′-AAGGGTGTAAAACGCAGCTC-3′), mouse *Samsn1* (F: 5′-TGCCTGCTCTCAGTTGTCTC-3′ and R: 5′-TCCGAAAACGGTCAAAATTC-3′), human *B2M* (F: 5′-AGGCTATC CAGCGTACTCCA-3′ and R: 5′-CGGCAGGCATACTCATCTTT-3′), and human *SAMSN1* (F: 5′-TCCCTCAAAGCCAGTGACTC-3′ and R: 5′-GCCACAGAATGGTCCTGAAT-3′). Changes in gene expression were calculated relative to β-actin or β_2-microglobulin using the $\Delta\Delta C_t$ method [23].

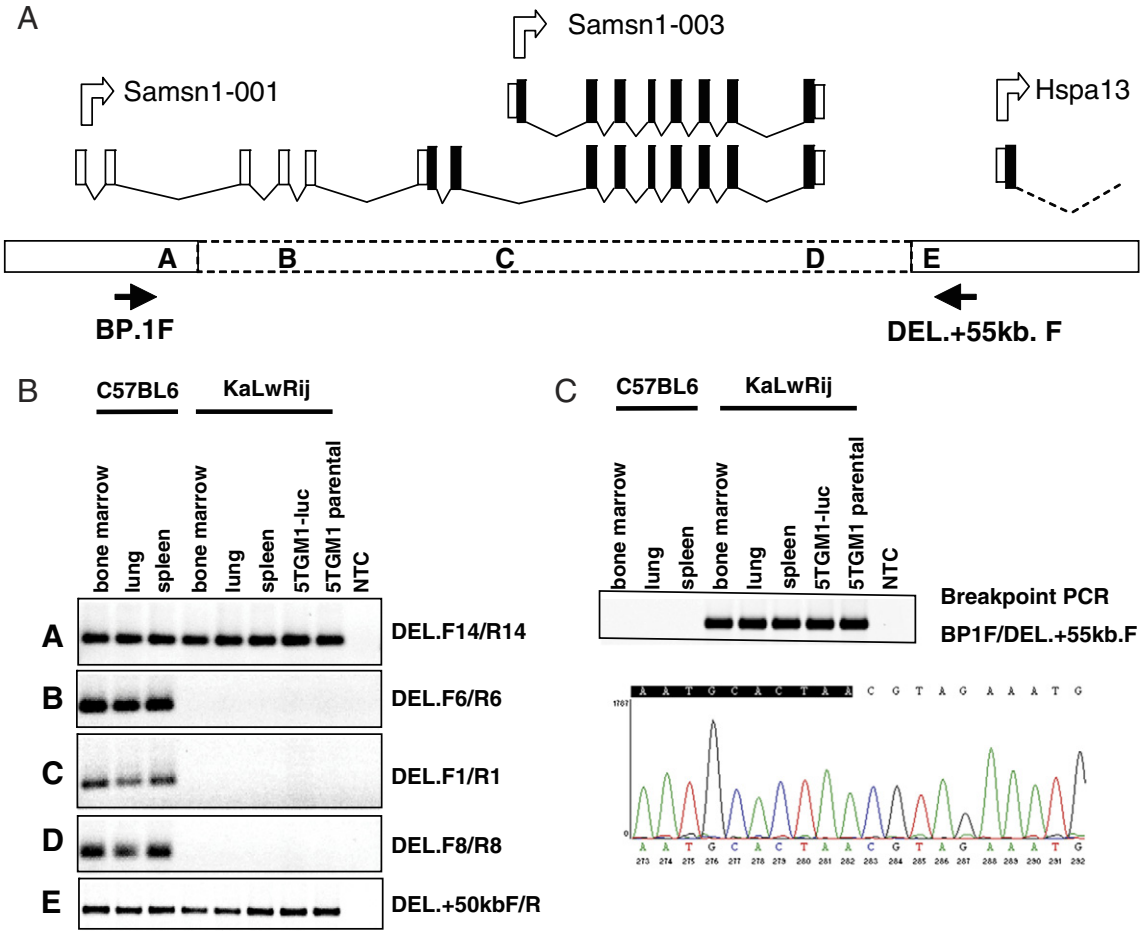

Figure 2. The *Samsn1* gene is deleted in C57BL/KaLwRij mice. (A) Extent of genomic deletion of the *Samsn1* gene in C57BL/KaLwRij mice. The two predominant protein coding isoforms from ensembl.org Mouse Genome Assembly are shown [Samsn1-001 (ENSMUST00000114240) and Samsn-003 (ENSMUST00000114239)]. Solid and open rectangles represent coding and non-coding exons, respectively. The large hatched horizontal rectangle at the bottom represents the genomic interval that is deleted, with the letters indicating the location of deleted (B–D) *versus* non-deleted (A and E) PCR primer binding sites. (B) PCR analysis of genomic DNA isolated from C57BL6 and C57BL/KaLwRij tissues/cell lines. Examples of PCRs that detect regions that are present (A and E) or deleted (B–D) in C57BL/KaLwRij tissues/cell lines are shown. The PCR primer names on the right-hand side correspond to those in Supplementary Table S1. NTC, no template (negative) control. (C) Breakpoint PCR with primer BP1F/DEL+55kb.F is only detectable in C57BL/KaLwRij-derived tissues or cell lines. The position of the breakpoint is indicated by the change from emboldened to normal text above the sequence chromatogram.

Flow Cytometry

Approximately 500 µl of peripheral blood was obtained from mice by cardiac puncture and collected in microfuge tubes containing 50 µl of 0.5 M EDTA. Femora and tibiae were flushed and BM cells were collected. Red blood cells were removed by hypotonic lysis and leukocytes were stained with phycoerythrin (PE)-Cy7–conjugated rat anti-mouse B220 (eBioscience, San Diego, CA), fluorescein isothiocyanate–conjugated rat anti-mouse CD3 (eBioscience), PE-Cy5–conjugated rat anti-mouse CD11b (BioLegend, San Diego, CA), APC-conjugated rat anti-mouse Gr1 (eBioscience), and PE-conjugated rat anti-mouse NK1.1 (BD Biosciences, San Jose, CA). FluoroGold (Life Technologies) was used to exclude dead cells. Cells were sorted on a FACSAria II (BD Biosciences) into B cell ($B220^{+}$), T cell ($CD3^{+}NK1.1^{-}$), monocyte ($CD11b^{hi}Gr1^{lo}$), and granulocyte ($CD11b^{hi}Gr1^{hi}$) populations for RNA extraction and real-time PCR. PCs were isolated from flushed long bones and identified using rat anti-mouse CD138 (R&D Systems, Minneapolis, MN) followed by PE-conjugated goat anti-rat IgG.

Deletion Mapping

Genomic DNA was isolated from mouse tissues using the DNeasy Blood and Tissue Kit (Qiagen) and PCRs were performed using AmpliTaq Gold Taq DNA Polymerase (Applied Biosystems, Foster City, CA), in accordance with the manufacturers' recommendations. Primers and annealing temperatures are indicated in Supplementary Table S1. PCR products spanning the breakpoint were cloned into pGEMT-Easy vector (Promega, Madison, WI) before sequencing.

Patient Samples

BM trephines were collected, with informed consent, from patients with MM or MGUS and from hematologically normal controls. All MM samples were collected from patients at diagnosis with no prior

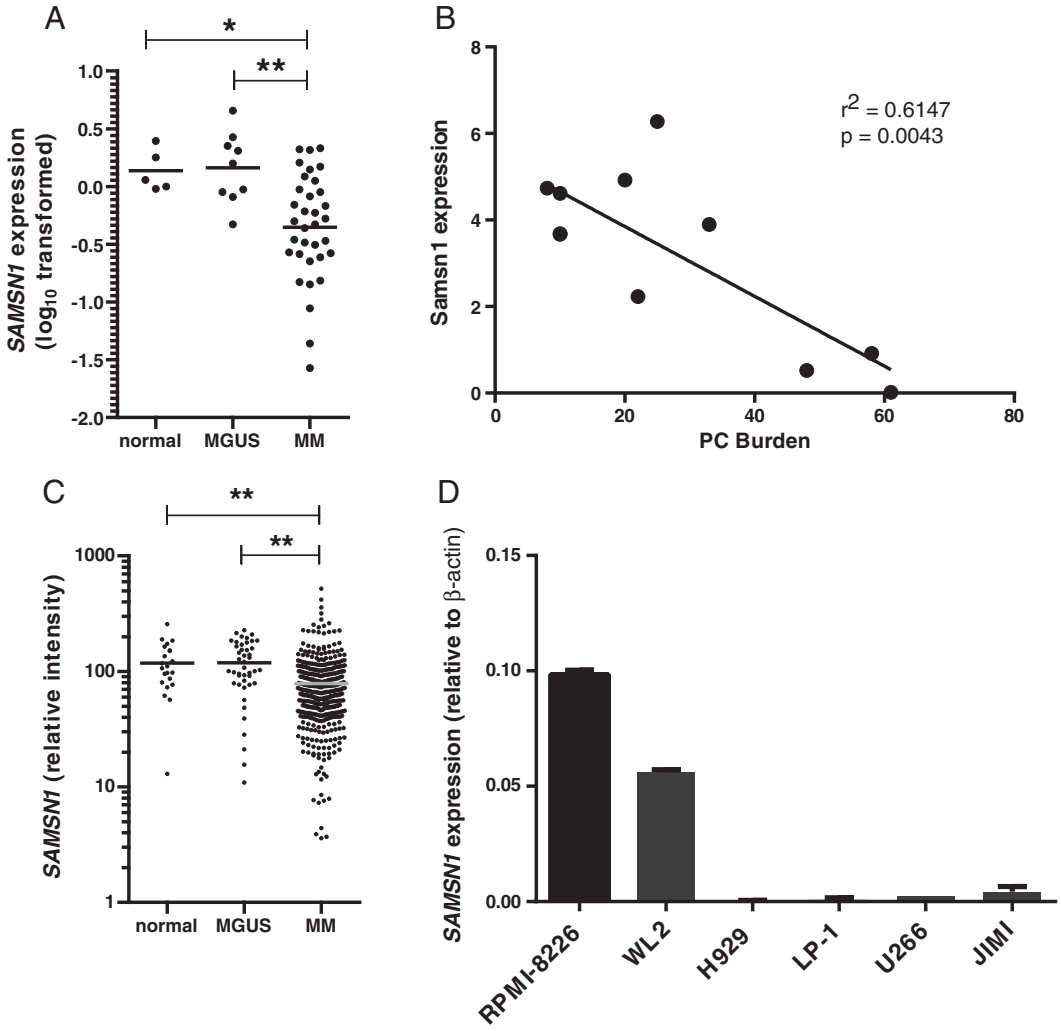

Figure 3. SAMSN1 expression is reduced in CD138+ PCs of patients with MM and HMCL. (A) *SAMSN1* expression (as determined by real-time PCR) is significantly reduced in the BMs of patients with MM ($n = 34$) compared with patients with MGUS ($n = 9$) and healthy age-matched controls ($n = 5$; $^*P < .05$, $^{**}P < .001$, one-way ANOVA with Tukey's multiple comparison test). (B) *SAMSN1* expression in CD138+ MACS isolated PCs from patients with MM negatively correlates with BM PC burden ($n = 10$, $r^2 = 0.6147$, $P = .0043$). (C) *In silico* analysis of published microarray data. $CD138^+$ PCs were isolated by MACS from 414 patients with MM, 44 patients with MGUS, and 22 age-matched controls. RNA was extracted and analyzed using the Affymetrix U133Plus2.0 microarray platform (GEO Accession Nos GSE4581 and GSE5900). Expression of *SAMSN1* is significantly reduced in PCs of patients with MM compared to those of patients with MGUS and normal controls. $P < 0.0001$, one-way ANOVA with Tukey's multiple comparison test. (D) Total RNA was extracted from six HMCLs and reverse transcribed. The levels of *SAMSN1* expression were assessed by real-time PCR.

therapy. This study was approved by the Royal Adelaide Hospital Human Research Ethics Committee.

CD138+ Magnetic-Activated Cell Sorting and RNA/DNA Isolation

CD138+ PCs were isolated from human BM samples from patients with MM (at diagnosis) using CD138 microbeads (Miltenyi Biotec, Auburn, CA) as per the manufacturer's instructions. Briefly, cryopreserved human BM samples (approximately 10^7 cells/ml) were thawed into 10 ml of Dulbecco's modified Eagle's medium (high glucose) with 15% fetal calf serum (FCS) and DNase. Sample was centrifuged at 300*g* for 10 minutes and the supernatant was aspirated. Cell pellet was resuspended in magnetic-activated cell sorting (MACS) buffer (2mM EDTA and 0.5% deionized BSA in phosphate-buffered saline) and CD138 microbeads were added. Cells/beads were incubated on ice for 15 minutes, washed in 1 ml of MACS buffer, and centrifuged at 300*g* for 10 minutes. Cells were resuspended in MACS buffer and applied to a pre-rinsed MS column. The column was washed three times with MACS buffer, followed by elution in 1 ml. The purity of final elution was determined by FACS analysis using a CD138-PE antibody and samples were confirmed to be >85% CD138+ following MACS. Total RNA and DNA were subsequently isolated using an All Prep DNA/RNA Micro Kit (Qiagen).

Cell Culture

Mouse 5TGM1 myeloma cells were maintained in Iscove's modified Dulbecco's medium (Sigma, St Louis, MO) with 20% FCS. HMCLs were maintained in RPMI-1640 medium (Sigma) with 10% FCS. BM stromal cells (BMSCs) were maintained in α-minimum essential medium (Sigma) with 10% FCS and 100 mM

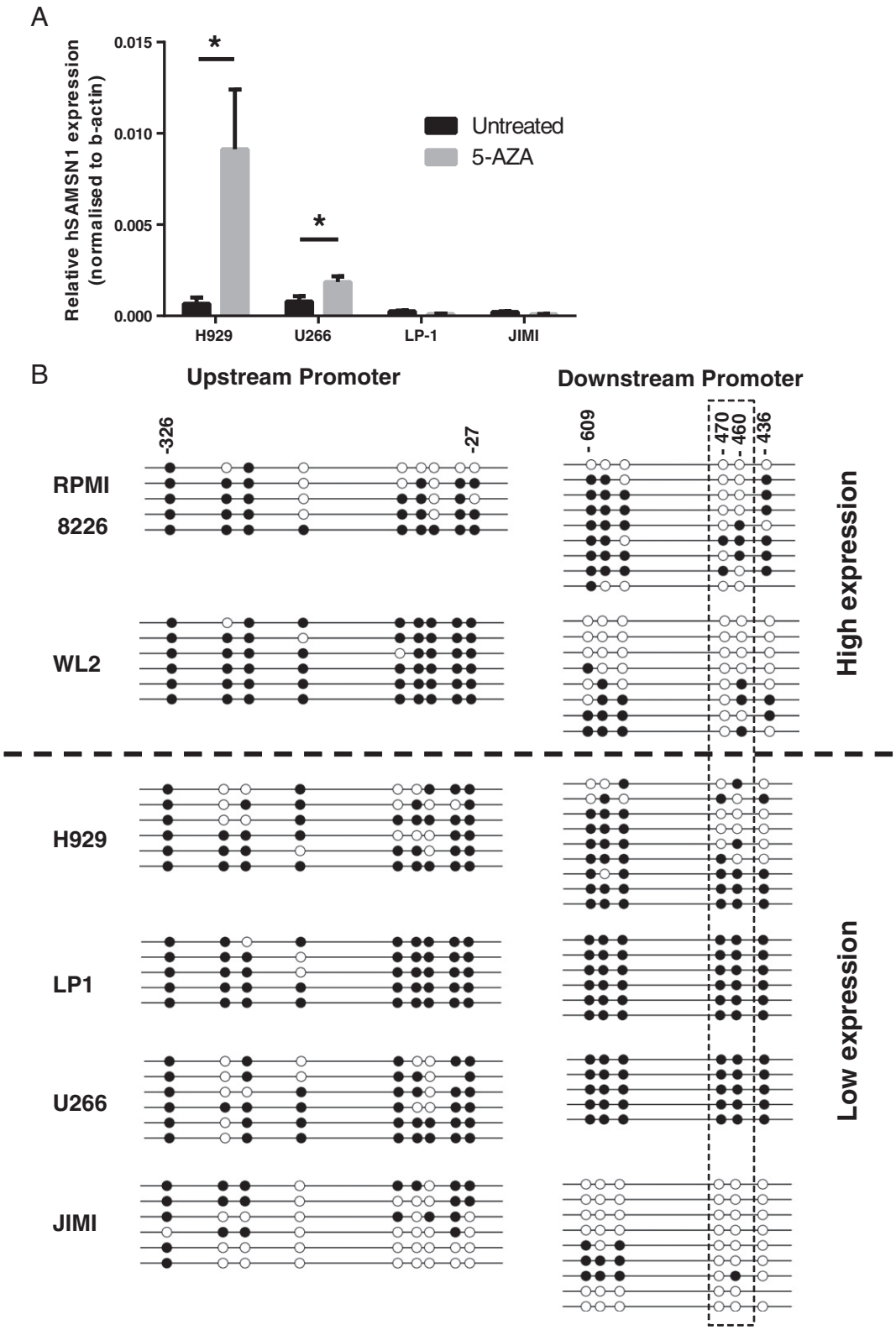

Figure 4. The *SAMSN1* gene is methylated in HMCLs. (A) H929, U266, LP-1, and JIMI cells were treated with 500 nM 5-aza-2′-deoxycytidine for 96 hours. Total RNA was isolated from treated and untreated controls. *SAMSN1* expression was significantly increased in response to 5-aza-2′-deoxycytidine treatment in the H929 and U266 cell lines, as determined by real-time PCR. *$P < .05$, *t* test. (B) *SAMSN1* promoter methylation in HMCLs. Patterns of CpG methylation revealed by sequencing of cloned PCR products for the two promoters of SAMSN1 are shown. Closed circles represent methylated CpGs and open circles represent unmethylated CpGs. The HMCLs are grouped according to SAMSN1 expression levels. The −470/−460 CpGs whose methylation status correlates with expression level are highlighted by the vertical hatched rectangle. The numbers above the CpGs are relative to the transcription start sites of the SAMSN1-001 (ENST00000285670) isoform for the upstream promoter and the SAMSN1-002 (ENST00000400566) and SAMSN1-002 (ENST00000400564) isoforms for the downstream promoter. SAMSN1 isoform data are from ensembl.org Human Genome Assembly GRCh37.p13.

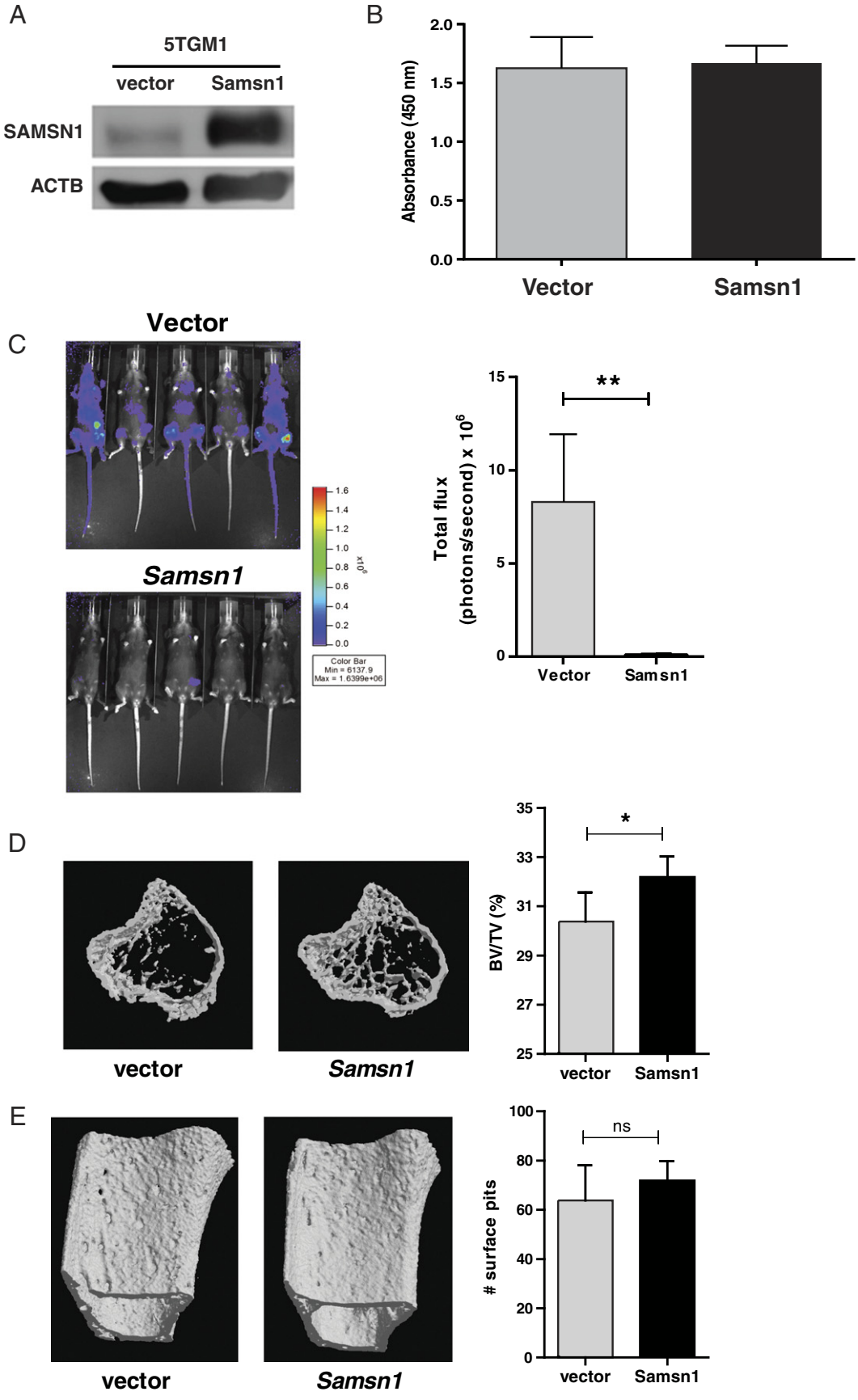
A
5TGM1
vector
Samsn1
SAMSN1
ACTB
B
Absorbance (450 nm)
2.0
1.5
1.0
0.5
0.0
Vector
Samsn1
C
Vector
Samsn1
1.6
1.4
1.2
1.0
0.8
0.6
0.4
0.2
0.0
x10^6
Color Bar
Min = 6137.9
Max = 1.6399e+06
Total flux
(photons/second) x 10^6
15
10
5
0
**
Vector
Samsn1
D
vector
Samsn1
BV/TV (%)
35
33
31
29
27
25
*
vector
Samsn1
E
vector
Samsn1
surface pits
100
80
60
40
20
0
ns
vector
Samsn1

L-ascorbate-2-phosphate. All culture media were supplemented with 2 mM L-glutamine, 100 U/ml penicillin, 100 μg/ml streptomycin, 1 mM sodium pyruvate, and 10 mM Hepes buffer (Life Technologies).

Methylation Analysis

Genomic DNA from myeloma cell lines was isolated using the DNeasy Blood and Tissue Kit (Qiagen). Two micrograms of DNA was bisulfite modified using the EpiTect Bisulfite Kit (Qiagen). Modified DNA was PCR amplified using EpiMark Hot Start Taq DNA Polymerase (New England Biolabs, Ipswich, MA) using the following primers: for downstream promoter: *SAMSN1.30mer.F1* (5′-AGTTATGTTTTTATTTATATTTAGAATGGG-3′) and Downstream.01.R (5′-TCACCCAAACTAAAATACAA TAACA-3′); for upstream promoter: *SAMSN1.BIS.*F (5′-TTG TTTTTATTTTGAGTTGTGTTTGT-3′) and SAMSN1.BIS.R (5′-ACTAAACTTCCTCCATTACTCTCTCTC-3′). PCR products were subcloned into pGemT-Easy vector (Promega) before sequencing. CpG methylation was assessed using QUMA (quma.cdb.riken.jp/).

Generation of Samsn1-Overexpressing Cell Lines

A luciferase-expressing 5TGM1 cell line (as described previously [24]) and an HMCL (H929)–overexpressing *Samsn1* were generated by infection with a retroviral vector (pRUFimCH2 or pRUFiG2, respectively) harboring a full-length cDNA encoding murine or human *Samsn1*. pRUFiG2 was generated from pRUF*neo* [25]. Briefly, oligonucleotides encoding *Not*I and *loxp* sequences were cloned into the *Cla*I site at the 5′ end of the *MC1Neo* gene. An oligonucleotide encoding an *loxp* sequence and a new multiple cloning site (including *Bam*HI, *Hpa*I, *Eco*RI, *Bgl*II, *Sac*II, *Sna*BI, *Nde*I, and *Xho*I) was cloned into the *Bam*HI site of pRUF*neo*. The *MC1Neo* gene was excised and replaced with an internal ribosome entry site, green fluorescent protein (*IRES-GFP*) cassette from pMSCV-IRES-GFP to generate pRUFiG2. To generate pRUFimCH2, the *IRES-GFP* cassette was excised from pRUFiG2 with *Xho*I and *Not*I and replaced with the *IRES-mCherry* cassette from pcDNA3-IRES-mCherry.

The full-length murine *Samsn1* cDNA was PCR amplified from a *Mus musculus* Samsn1 cDNA clone (clone 30077237; Open Biosystems, Huntsville, AL) and subcloned into pRUFimCH2 to generate pRUFimCH2-*Samsn1*. The full-length human SAMSN1 cDNA was PCR amplified from a *Homo sapiens SAMSN1* cDNA clone (clone 4343284; Open Biosystems) and subcloned into pRUF-iG2 to generate pRUF-iG2-*SAMSN1*. Retroviral vectors were transfected into HEK-293T cells and viral particle-containing supernatant was used to infect 5TGM1-luc cells or H929 cells, as previously described [26]. Cell lines were sorted on a Beckman Coulter Epics Altra HyperSort, using Expo MultiComp Software version 1.2B (Beckman Coulter, Miami, FL) and pooled cell lines were established from the top 30% of mCherry or GFP-expressing cells. Resultant Samsn1-overexpressing cell lines (and empty vector controls) were used for subsequent *in vitro* and *in vivo* assays.

Western Blot

5TGM1 cells (2×10^7) were lysed in 1 ml of lysis buffer containing 1% NP-40, 20 mM Hepes, 150 mM NaCl, 10% glycerol, 2 mM Na_3VO_4, 10 mM $Na_4P_2O_7$, 2 mM NaF, and Complete EDTA-free Protease Inhibitor Cocktail (Roche, Mannheim, Germany). One hundred micrograms of lysate was loaded on a 10% acrylamide gel and subjected to sodium dodecyl sulfate–polyacrylamide gel electrophoresis. Proteins were transferred to polyvinylidene difluoride membrane overnight and the membrane was subsequently incubated at room temperature in blocking buffer [Tris-buffered saline containing 0.1% Tween 20 and 2.5% ECL Blocking Agent (GE Healthcare, Little Chalfont, United Kingdom)] for 6 hours. The membrane was incubated overnight at 4°C with rabbit polyclonal anti-SAMSN1 antibody (Sigma) diluted 1:500 in blocking buffer, followed by alkaline phosphate-conjugated anti-rabbit IgG (Millipore, Billerica, MA) diluted 1:2500 in blocking buffer for 1 hour at room temperature. Proteins were visualized using ECL detection reagent (GE Healthcare) on a Typhoon FLA 7000 IP[2] (GE Healthcare).

5-Aza-2′-Deoxycytidine Treatment in HMCL

HMCLs were seeded at 2×10^5 cells/ml and treated with 500 nM 5-aza-2′-deoxycytidine (Life Technologies) diluted in culture medium for 96 hours, replenishing treatment media daily. Total RNA was isolated from treated cells and untreated controls and specific gene expression was determined by real-time PCR.

Adhesion Assays

BMSCs were seeded at 8×10^3 cells per well in a 96-well plate and allowed to adhere overnight. Empty wells (plastic) were used as controls for adhesion. H929 or 5TGM1 cells (expressing an empty vector control or SAMSN1) were seeded at 2×10^4 cells per well in 100-μl volume and incubated for 10 minutes at 37°C with 5% CO_2. Cells were gently aspirated followed by three washes with 100 μl of HBSS with 5% FCS to remove non-adherent cells. One hundred microliters of standard culture medium was added to each well and four images taken per well at ×10 magnification. The number of GFP-positive cells per field of view was determined using FIJI analysis software (http://fiji.sc).

Proliferation Assays

5TGM1 cells were seeded at 2000 cells per well in triplicate in a 96-well plate. BrdU (Roche) was added to the cells and incubated for 24 hours at 37°C with 5% CO_2. Cells were fixed and stained as per the manufacturer's protocol and absorbance was measured at 450 nm.

BMSCs were seeded at 5×10^4 cells per well in a 96-well plate (black plate with clear, flat bottom; Corning Life Science, Pittston, PA) in 100

Figure 5. Overexpression of *Samsn1* completely inhibits MM tumor growth *in vivo*. (A) Western blot for Samsn1 in 5TGM1-vector and 5TGM1-*Samsn1* cells. (B) No significant difference was seen in the proliferation of 5TGM1-vector and 5TGM1-*Samsn1* cells as determined by BrdU incorporation. (C) C57BL/KaLwRij mice were injected intravenously with 5×10^5 5TGM1 cells. On day 28, mice received luciferin intraperitoneally and tumor growth was assessed using the Xenogen IVIS 100. Bioluminescence images of tumor growth in mice receiving control (upper panel) and *Samsn1*-expressing (lower panel) 5TGM1 cells ($n = 5$ per group) are shown. The *in vivo* growth of *Samsn1*-expressing 5TGM1 cells is significantly reduced compared to control cells as determined by quantification of photon flux. $^{**}P = .0079$, Mann-Whitney *U* test. (D) Representative three-dimensional images of the tibial trabecular structure of tumor-bearing mice. Osteolysis was significantly lower in mice carrying 5TGM1-Samsn1 tumors as determined by bone volume analysis ($^{*}P = .0244$, *t* test, $n = 5$). (E) Representative three-dimensional images of the tibial cortical structure of tumor-bearing mice. There was no significant difference in the number of cortical pits.

μl of α-minimum essential medium with 10% FCS and allowed to adhere overnight. The medium was aspirated and 5TGM1-Samsn1 or 5TGM1-vector cells were seeded (in triplicate) at 5×10^3 cells per well in 100 μl of Iscove's modified Dulbecco's media + 20% FCS. Cells were incubated for 3 days at 37°C with 5% CO_2. Bioluminescence was determined using the Xenogen IVIS 100 Bioluminescence Imaging System (Caliper Life Sciences, Hopkinton, MA), following addition of 100 μl of 300 ng/ml luciferin per well and analysis using Living Image software (PerkinElmer, Waltham, MA). Absolute cell number per well was determined using a standard curve for bioluminescence.

Animals

C57BL/6 and C57BL/KaLwRij mice were bred and housed at the Institute of Medical and Veterinary Science Animal Care Facility. Animal studies were approved by the Institute of Medical and Veterinary Science/Adelaide Health Service and University of Adelaide Animal Ethics Committees. C57BL/KaLwRij mice (aged 6-8 weeks) received 5×10^5 luciferase-expressing 5TGM1 cells in 100 μl of sterile phosphate-buffered saline through the tail vein. At weekly intervals, mice were administered 150 mg/kg luciferin intraperitoneally and imaged using the Xenogen IVIS 100 Bioluminescence Imaging System until termination of the experiment at day 28. Tumor burden was quantitated using Living Image software.

μ-CT Analysis

Bone volume was evaluated using μ-CT (Skyscan 1174 X-ray Microtomograph; Bruker MicroCT, Kontich, Belgium). All tibiae were scanned at 48 kV/800 μA, with an isometric resolution of 6.49 μm/pixel using a 0.25-mm aluminium filter and two-frame averaging. Reconstruction of the original scan data was performed using NRecon. Analysis of bone volume fraction (BV/TV) was performed using CTAn. A total of 300 slices (1.947 mm) was analyzed for each tibia, commencing 85 slices (0.552 mm) distal to the growth plate. Digital segmentation of the bone from air/tissues was performed by adaptive (median-C) thresholding. The volume of interest were reconstructed in three dimensions using ANT software.

Statistical Analysis

Statistical analysis was performed using GraphPad Prism version 5.02 for Windows (GraphPad Software, San Diego, CA; www.graphpad.com). Variance between patient groups was compared using analysis of variance (ANOVA) with Tukey's multiple comparison test. Differences in tumor burden were compared between groups using a Mann-Whitney *U* test. *In vitro* assays were analyzed using *t* tests or ANOVA as appropriate. A *P* value of .05 was considered statistically significant.

Results

Samsn1 Expression Is Significantly Reduced in C57BL/KaLwRij Mice

To identify factors that may contribute to the development of MM, we compared the gene expression profiles from the closely related C57BL/6 and C57BL/KaLwRij mouse strains. While both the C57BL/6 and C57BL/KaLwRij strains have been demonstrated to develop monoclonal gammopathy at a similar rate (60-70% by 2 years old) [27,28], the C57BL/KaLwRij mice are unique in their ability to spontaneously develop MM at a low frequency (0.5% of mice > 2 years old). Furthermore, the C57BL/KaLwRij strain allows the successful engraftment of exogenous murine myeloma PCs, while the C57BL/6 strain does not [16,17,29]. The C57BL/KaLwRij model is one of the most widely studied preclinical animal models of MM and the MM disease exhibited by these animals faithfully recapitulates the symptoms of the human disease, including osteolysis [16,30–32]. In addition, these animals have previously been used to identify factors that play a role in the pathogenesis of human MM [33,34].

Total RNA was extracted from the long bones (tibiae and femora) of age- and sex-matched C57BL/6 and C57BL/KaLwRij mice. Expression profiling of the long bones revealed a small number of genes (87) that are differentially expressed between the two strains by two-fold or more (Figure 1*A*). Of these, 22 were unnamed genes with no identified function and a further 7 had no human orthologue. Literature searches were conducted for the remaining 58 genes (Table 1) and these were subsequently prioritized for further investigation based on their potential relevance to MM. Statistically significant differences in expression were confirmed by quantitative PCR for 5 of the 20 most promising candidates (data not shown). Of particular interest was the expression of *Samsn1*, which was shown to be absent in the bone of C57BL/KaLwRij mice at both the mRNA and protein levels (Figure 1*B*). *Samsn1* has been shown to play a role in regulating adaptive immune responses and the development of B cells [19,20], which, coupled with our microarray data, highlighted *Samsn1* as a promising candidate for further investigation into its potential role in the development of MM.

Loss of SAMSN1 Is a Feature of the 5TGM1/C57BL/KaLwRij Mouse Model of MM

To identify whether *Samsn1* may play a role in the development of MM in the mouse model, we first investigated *Samsn1* mRNA expression in various tissues and found it to be consistently absent within the C57BL/KaLwRij mice compared to C57BL/6 controls (Figure 1*C*). Previous studies have shown that *Samsn1* is expressed in cells of the hematopoietic compartment [18]. As such, hematopoietic cell subsets (B cells, T cells, monocytes, granulocytes, PCs, and stromal cells) were isolated by FACS and *Samsn1* expression was evaluated by real-time PCR. As seen in Figure 1*D*, *Samsn1* mRNA expression was absent across the entire range of hematopoietic cell subsets, including PCs, the effector cells of MM. Notably, this lack of *Samsn1* expression was also evident in the well-characterized 5TGM1 cell line (Figure 1*E*), a finding consistent with its C57BL/KaLwRij origin. From these findings, we hypothesized that the absence of *Samsn1* expression in these mice, and specifically within the malignant 5TGM1 PCs, may represent a crucial mechanism by which MM disease develops in this murine model.

The Samsn1 Gene Is Deleted in C57BL/KaLwRij Mice and 5TGM1 Murine PCs

To identify a mechanism for the global lack of *Samsn1* expression in the C57BL/KaLwRij mice, we attempted to PCR amplify the two promoter regions of *Samsn1* to analyze this region for CpG methylation (see Figure 2*A* for overview of the gene structure). Interestingly, using primers designed specifically to the downstream promoter region of the *Samsn1* gene, we were unable to amplify the genomic DNA from tissues derived from the C57BL/KaLwRij mice (data not shown). Upon further analysis, we identified a large chromosomal deletion, encompassing the entire coding region of the *Samsn1* gene in the C57BL/KaLwRij mice. Notably, the corresponding region in the C57BL/6 control strain was not deleted (Figure 2B, Supplementary Table S1, Supplementary Figure S1). PCR performed

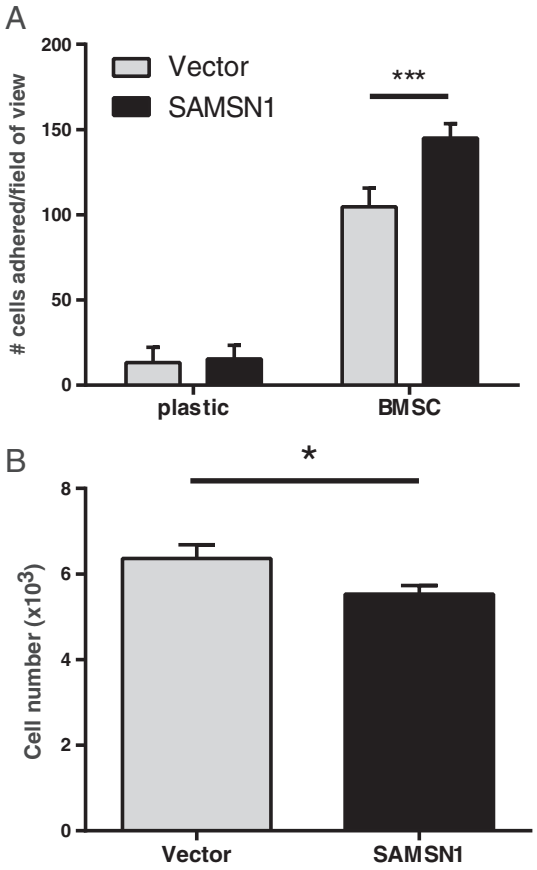

Figure 6. Overexpression of *Samsn1* increases adhesion and decreases cell growth on stroma *in vitro*. (A) 5TGM1-Samsn1 or -vector control cells were allowed to adhere to a monolayer of BMSCs for 10 minutes, followed by gentle washing to remove non-adherent cells. The number of GFP + adherent cells was determined using FIJI analysis software. Mean ± SEM, $n = 4$, ***$P < .001$, *t* test. (B) Equal numbers of 5TGM1-Samsn1 or -vector control cells were seeded on BMSC and the total number of cells after 72 hours was determined by bioluminescence imaging techniques. Mean ± SEM, $n = 3$, *$P <. 05$, paired *t* test.

with primers BP.1F and DEL+55kb.F, which flank the deletion interval (Figure 2*A*), only yielded a product with KaLwRij-derived genomic DNA (Figure 2*C*). Sequencing of this PCR product revealed that the deletion is 179,971 bp in length and extends from midway through intron 2 to an intergenic region between *Samsn1* and the next nearest downstream gene, *Hspa13*. The deleted region extends from 75,816,191 to 75,996,161 of mouse chromosome 16, and the three genes *Hspa13*, *Rbm11*, and *Lipi* that are located immediately downstream of *Samsn1* were not deleted (data not shown; Supplementary Table S1). Notably, the 179,971 bp deletion was also shown to be present in the 5TGM1 malignant PC line (Figure 2, *B* and *C*). These data indicate that the C57BL/KaLwRij mice are genetically null for *Samsn1*. This model of MM therefore does not express *Samsn1* in the microenvironment or in the malignant PCs and therefore provides an ideal model through which to investigate the role of PC-specific *Samsn1* expression in MM disease development *in vivo*.

Samsn1 Expression Is Reduced in a Subset of Patients with MM

To ascertain whether *SAMSN1* is also aberrantly expressed in patients with MM, RNA was extracted from total BM trephine biopsies recovered from patients with MM ($n = 34$) and MGUS ($n = 9$) at diagnosis and from hematologically normal, age-matched controls ($n = 5$). *SAMSN1* expression was shown to be significantly reduced in the BMs of patients with MM when compared with those of patients with MGUS and age-matched controls ($P = .0019$, one-way ANOVA; Figure 3*A*). We next wanted to investigate the PC-specific expression of *SAMSN1* in patients with MM. Therefore, we specifically isolated CD138 + PCs from BM samples of patients with MM using MACS techniques and were subsequently able to determine that patients presenting with higher BM PC burden at diagnosis had significantly lower PC-specific *SAMSN1* expression ($n = 10$, $r^2 = 0.6147$, $P = .0043$; Figure 3*B*). In support of our findings, *in silico* analyses of publicly available data sets from large-scale microarray studies (GEO Accession Nos GSE4581 and GSE5900; Myeloma Institute, University of Arkansas) also showed that *SAMSN1* mRNA expression was significantly reduced in purified PCs from patients with MM ($n = 414$) compared with patients with MGUS ($n = 44$) and healthy age-matched controls ($n = 22$; $P < .0001$, one-way ANOVA; Figure 3*C*). Interrogation of these data sets revealed that approximately 25% of patients with MM express *SAMSN1* below the normal range compared to only 7% of patients with MGUS. Low *SAMSN1* expression was also observed in four of six HMCLs examined (Figure 3*D*). Together, these data suggest that there is a significant reduction in *SAMSN1* expression in myeloma PC.

The Samsn1 Promoter Is Methylated in HMCLs

Despite its reduced expression levels in lung cancer cell lines [21], methylation of the *SAMSN1* promoter has not been previously

investigated in the context of human disease. We hypothesize that, due to the significant reduction of *SAMSN1* expression in patients with MM and HMCLs, *SAMSN1* expression may be modulated by differential methylation of the promoter. In support of this, a recent study by Heller et al. listed *SAMSN1* as a significantly upregulated gene in two myeloma cell lines following treatment with the DNA methyltransferase inhibitor 5-aza-2′-deoxycytidine [35]. Consistent with these findings, we showed an increase in mRNA expression of *SAMSN1* in two HMCLs (U266 and H929) following treatment with 500 nM 5-aza-2′-deoxycytidine for 96 hours (Figure 4*A*). Interestingly, although displaying similar low basal *SAMSN1* expression levels, the JIMI and LP-1 cell lines did not exhibit an increase in *SAMSN1* expression following treatment with 5-aza-2′-deoxycytidine (Figure 4*A*).

To investigate this further, we examined the methylation pattern of the *SAMSN1* promoter region in a panel of HMCLs using bisulfite-sequencing techniques. Similar to its mouse orthologue, the human *SAMSN1* gene has two promoter regions associated with the full-length protein coding isoforms (see Figure 2*A*). As seen in Figure 4*B* (*left panel*), there is evidence of high levels of methylation of the CpG dinucleotides in the upstream *SAMSN1* promoter region of all HMCLs screened. In contrast, the downstream *SAMSN1* promoter exhibited differential methylation, particularly in the two central CpGs at −470 and −460 relative to the transcription start site (Figure 4*B*, *right panel*, *hatched box*). Importantly, the degree of methylation of the −470 and −460 CpGs of the downstream promoter corresponded with *SAMSN1* expression levels in the HMCLs, with the lowest levels of combined methylation of these two CpGs seen in the RPMI-8226 (28%) and WL-2 (19%) cell lines, which show the greatest expression of *SAMSN1* (see Figure 3*D*). In contrast, H929 (56%), U266 (100%), and LP-1 (100%) cells exhibit higher degrees of methylation at the −470 and −460 CpGs and do not express *SAMSN1*. Consistent with the lack of induction of *SAMSN1* expression following treatment with 5-aza-2′-deoxycytidine, JIMI cells exhibit −470/−460 CpG methylation levels equivalent to that seen in the RPMI-8226 and WL-2 cell lines (5%). Interestingly, although displaying low basal *SAMSN1* expression and a high degree of promoter methylation, the LP-1 cell line also did not respond to 5-aza-2′-deoxycytidine treatment. These data suggest a role for promoter methylation in the modulation of *SAMSN1* expression and also highlight the existence of alternative, yet to be defined, mechanisms.

Overexpression of Samsn1 in 5TGM1 Cells Completely Inhibits MM Disease Development In Vivo

As detailed above, our studies show that *Samsn1* expression is absent in the 5TGM1/C57BL/KaLwRij mouse model of myeloma, and this is consistent with reduced expression in a subset of patients with MM. We next aimed to determine whether restoration of *Samsn1* expression in the 5TGM1 cells affects the development of MM *in vivo*. Luciferase-expressing 5TGM1 cells (which do not express Samsn1; see Figure 1*E*) were transduced with a Cherry-labeled *Samsn1* expression construct (5TGM1-Samsn1) or vector control (5TGM1-vector), and *Samsn1* expression was confirmed by real-time PCR (data not shown) and Western blot (Figure 5*A*). The expression of Samsn1 in 5TGM1-Samsn1 cells was equivalent to levels seen in PC isolated from C57BL/6 mice (data not shown). The use of luciferase-labeled cells allowed us to track the progression of MM disease spread and development *in vivo* using bioluminescence imaging techniques [24,34].

Re-expression of *Samsn1* in 5TGM1 cells had no effect on their proliferative capacity *in vitro*, as determined by a BrdU incorporation assay (Figure 5*B*). However, re-introduction of Samsn1 to the 5TGM1 cells was found to significantly inhibit the development of MM disease *in vivo*, as seen by a significant decrease in bioluminescence of 5TGM1-Samsn1–inoculated mice compared to the 5TGM1-vector controls (P = .0079, Mann-Whitney U test; Figure 5*C*). In keeping with the absence of tumor in mice inoculated with 5TGM1-Samsn1 cells, the bone volume fraction in the tibiae of these animals was significantly greater than that of control tumor-bearing mice (32.18 ± 0.3815% compared with 30.38 ± 0.5256%, P = .0244, two-tailed t test; Figure 5*D*). While the number of resorption lacunae that traversed the cortices of the tibiae of both groups was similar (63.8 ± 6.402 compared with 71.9 ± 3.519, P = .2998; Figure 5*E*), the resorption lacunae in the 5TGM1-*Samsn1* group tended to be smaller. These data indicate that restoring expression of *Samsn1* in the murine 5TGM1 PCs can completely abolish the capacity of these cells to form intramedullary tumors *in vivo* and therefore prevents the osteolysis that is commonly observed in this tumor model in response to MM.

SAMSN1 Overexpression Reduces Cell Growth in the Presence of BMSCs In Vitro

To determine a mechanism by which *Samsn1* expression may inhibit the development of MM, we investigated the adhesive properties of the vector- and Samsn1-expressing cells *in vitro*. 5TGM1-Samsn1 cells exhibited an increased capacity to adhere to a BMSC layer compared to the 5TGM1-vector control cells in a short-term *in vitro* adhesion assay (Figure 6*A*). This was confirmed in the H929 HMCL (Supplementary Figure S2). As adherence of cells of the hematopoietic lineage to stroma has previously been demonstrated to reduce proliferation [36–38], we next wanted to ascertain whether this increase in adhesion was associated with an altered proliferative capacity of the 5TGM1-Samsn1 cells. 5TGM1-Samsn1 and 5TGM1-vector cells were grown in the presence of BMSC and total cell number was quantified after a 72-hour incubation period. The total number of 5TGM1-Samsn1 cells was reduced compared to the vector control cells (Figure 6*B*), suggesting that the expression of *Samsn1* in PCs may play a role in regulating cell adhesion and proliferation, thereby accounting for the lack of tumor growth observed *in vivo*.

Discussion

This is the first study to identify a key genetic variation, specifically the deletion of the *Samsn1* gene, in the C57BL/KaLwRij mice, which may contribute to the propensity of these mice to spontaneously develop myeloma-like disease. Moreover, analysis of patient data showed that while expressed in PCs from healthy donors and patients with MGUS, *SAMSN1* expression is significantly reduced in patients with MM suggesting a role for SAMSN1 in MM disease development and/or progression. Furthermore, we also showed that restoration of *Samsn1* expression in MM PCs inhibited myeloma disease development *in vivo,* highlighting a potential tumor suppressor role for this protein in MM.

Although loss of heterozygosity at the chromosomal region 21q11-21, which includes the *SAMSN1* gene, has previously been associated with lung cancer development [21], this is the first study in which *SAMSN1* has been shown to play a tumor suppressor role in a hematological malignancy. Interestingly, this chromosomal region has also been identified as a region of frequent translocation events in hematological

malignancies [39] and more recently was identified specifically as a region of chromosomal gain in a small number of patients with MM [40]. Furthermore, studies have previously shown an increase in *SAMSN1* expression both in PC leukemia and MM [18,41]. The contradiction between these studies and our own findings can likely be attributed to the large degree of genetic heterogeneity observed in patients with MM. Indeed, the study by Ni et al. identified a gain of 21q (specifically associated with a gain of *SAMSN1*) in only a very small number of patients on the background of a BCL1/JH t(11;14) (q13;q32) translocation, while we observe significantly reduced *SAMSN1* expression in an unbiased sample of total BM trephines from patients with MM compared to healthy donors. Furthermore, our findings are supported by preliminary *in silico* analysis of the University of Arkansas gene expression data set with approximately 25% of MM patient–derived PC expressing *SAMSN1* below the normal range. Further *in silico* analysis also suggests that reduction of *SAMSN1* is not associated with any particular MM genetic subtype. Rather, patients with low *SAMSN1* expression can be found in most subgroups. However, within each subgroup, these patients tend to have poorer disease-related survival compared to patients with *SAMSN1* expression levels in the normal range (data not shown). This is also consistent with the correlation observed between increased BM PC burden and low CD138+ PC-specific *SAMSN1* expression. It will be important in the future to determine what common genetic anomalies may be associated with reduced *SAMSN1* expression in patients, e.g., activated nuclear factor kappa B pathway signaling, deregulated *MYC*, or common translocations, which may account for the enhanced severity of disease. It will also be necessary to dissect out whether these genetic signatures are the cause or consequence of reduced *SAMSN1* expression.

Although Yamada et al. demonstrated frequent down-regulation of *SAMSN1* in lung cancer cell lines, no mechanism for this down-regulation was identified [21]. A number of recent studies have shown global hypomethylation of the genome to be associated with the progression of MM disease from the non-malignant MGUS stage, with the majority of this hypomethylation occurring outside of defined CpG islands [15,42,43]. Gene-specific hypermethylation, associated with CpG islands within promoter regions, is also evident in MM progression. This hypermethylation has, to date, largely been associated with genes involved in developmental processes, cell cycle, and regulation of transcription [15,43]. In this study, we present *SAMSN1* as a novel gene exhibiting hypermethylation in cell lines derived from patients with MM. We have correlated differential methylation of specific CpGs within the downstream *SAMSN1* promoter with gene expression levels. Furthermore, we demonstrated an increase in *SAMSN1* expression in HMCLs following treatment with the DNA methyltransferase inhibitor 5-aza-2′-deoxycytidine. This is supported by a previous study showing a significant increase in *SAMSN1* expression in an HMCL upon treatment with 5-aza-2′-deoxycytidine [35]. This finding provides evidence of *SAMSN1* hypermethylation and subsequent down-regulation as a potential marker of MM disease.

C57BL/KaLwRij and C57BL/6 are closely related strains of mice. The C57BL/KaLwRij strain uniquely exhibits an inherent ability to develop MM disease as well as permitting the growth of the exogenous 5T series of mouse MM lines, while the C57BL/6 strain does not [16,17,29]. The 5TGM/C57BL/KaLwRij model provided an ideal opportunity to investigate the effect of PC-specific *Samsn1* expression on the *in vivo* development of MM, as we have shown a large genomic deletion within chromosome 16, encompassing the entire *Samsn1* coding region, resulting in an animal that is null for *Samsn1* expression. As this deletion was shown to be specific to the C57BL/KaLwRij strain, we hypothesized that the deletion of *Samsn1* was necessary but not sufficient for the unique development of MM in these animals. Despite being Samsn1 null, C57BL/KaLwRij mice only develop MM at a very low rate (approximately 0.5% greater than 2 years old) [16], suggesting that the loss of Samsn1 alone is not sufficient to drive the development of this disease. It is therefore likely that the 5TGM1 cells contain further genetic or epigenetic alterations that, in combination with the loss of *Samsn1*, account for the malignancy in this system.

It is evident that the PC-specific loss of *Samsn1* expression is critical in the development of MM, as restoration of *Samsn1* expression in the 5TGM1 cell line significantly inhibited disease development *in vivo*. In keeping with this finding, *SAMSN1* expression is significantly reduced both in a subset of HMCLs and within CD138+ purified PCs from BMs of patients with MM. Together, these data suggest that the role of SAMSN1 in MM development is likely to be largely PC-specific.

Although the precise cellular function of SAMSN1 is largely unknown, it has been reported to be expressed primarily in the hematopoietic compartment [18] and to be up-regulated by B cell stimulators resulting in the activation and differentiation of B cells [20]. In addition, overexpression of *Samsn1* in murine splenic B cells resulted in inhibition of proliferation, while mice with knock-out *Samsn1* showed increased proliferation of naïve B cells [19,20]. Collectively, these data support a role for SAMSN1 in B cell development and function. In addition, a role for SAMSN1 in actin cytoskeleton organization and B cell spreading has also been proposed [44]. Our preliminary findings suggest that expression of SAMSN1 in myeloma cell lines results in increased adhesion to BMSCs and subsequent decreased cell growth in short-term *in vitro* assays, accounting for the reduced tumor growth observed *in vivo*. This is in contrast to cells grown in the absence of BMSC wherein no change in proliferation is observed. These findings are supported by previous studies that have demonstrated a link between increased adhesion of hematopoietic progenitor cells to stroma and decreased cellular proliferation [36,37]. In addition, specific binding of hematopoietic progenitor cells through the cell adhesion molecule PSGL-1 has been associated with suppressed cellular proliferation [45] and adhesion of lymphoma cells to BMSCs results in G_1 arrest [38]. Taken together, these data implicate SAMSN1 as not only a modulator of B cell development and function [19,20,44] but also a protein that plays a role in controlling cell adhesion and proliferation of PCs within the BM microenvironment. However, it remains to be fully elucidated as to how loss of SAMSN1 contributes to MM development and this requires further investigation.

The structural nature of SAMSN1, specifically the presence of SH3 and SAM domains, places it in the class of intracellular adaptor molecules [46,47]. Therefore, it is probable that key interactions and signaling pathways are modulated through SAMSN1 and the deregulation of these pathways contributes to the development of MM. Further investigation is required to identify a mechanism of action for SAMSN1 in suppressing MM tumor development, including potentially important interacting partners and downstream activated and/or repressed pathways.

Conclusions

In summary, we have identified *Samsn1* as an MM tumor suppressor gene with reduced *SAMSN1* expression observed both in the C57BL/KaLwRij

mouse model of MM and a proportion of patients with MM. Further studies of the prognostic significance of reduced *SAMSN1* expression in patients with MM are warranted. Identification of differential methylation of the *SAMSN1* promoter suggests that demethylating agents may be clinically useful in the treatment of MM. Furthermore, investigation into the biologic outcomes of SAMSN1 molecular interactions may reveal novel therapeutic targets for the treatment of MM. Finally, further analysis of the C57BL/KaLwRij genome may provide key insights into genes that may be involved in the initiation and/or progression of MM disease.

Supplementary data to this article can be found online at http://dx.doi.org/10.1016/j.neo.2014.07.002.

References

[1] Siegel R, Naishadham D, and Jemal A (2012). Cancer statistics, 2012. *CA Cancer J Clin* **62**, 10–29.

[2] Brenner H, Gondos A, and Pulte D (2009). Expected long-term survival of patients diagnosed with multiple myeloma in 2006-2010. *Haematologica* **94**, 270–275.

[3] Weiss BM, Abadie J, Verma P, Howard RS, and Kuehl WM (2009). A monoclonal gammopathy precedes multiple myeloma in most patients. *Blood* **113**, 5418–5422.

[4] Rajkumar SV, Kyle RA, and Buadi FK (2010). Advances in the diagnosis, classification, risk stratification, and management of monoclonal gammopathy of undetermined significance: implications for recategorizing disease entities in the presence of evolving scientific evidence. *Mayo Clin Proc* **85**, 945–948.

[5] Kyle RA, Therneau TM, and Rajkumar SV, et al (2002). A long-term study of prognosis in monoclonal gammopathy of undetermined significance. *N Engl J Med* **346**, 564–569.

[6] Fonseca R, Bergsagel PL, and Drach J, et al (2009). International Myeloma Working Group molecular classification of multiple myeloma: spotlight review. *Leukemia* **23**, 2210–2221.

[7] Facon T, Avet-Loiseau H, and Guillerm G, et al (2001). Chromosome 13 abnormalities identified by FISH analysis and serum beta2-microglobulin produce a powerful myeloma staging system for patients receiving high-dose therapy. *Blood* **97**, 1566–1571.

[8] Jenner MW, Leone PE, and Walker BA, et al (2007). Gene mapping and expression analysis of 16q loss of heterozygosity identifies WWOX and CYLD as being important in determining clinical outcome in multiple myeloma. *Blood* **110**, 3291–3300.

[9] Avet-Loiseau H, Attal M, and Moreau P, et al (2007). Genetic abnormalities and survival in multiple myeloma: the experience of the Intergroupe Francophone du Myelome. *Blood* **109**, 3489–3495.

[10] Fonseca R, Van Wier SA, and Chng WJ, et al (2006). Prognostic value of chromosome 1q21 gain by fluorescent in situ hybridization and increase CKS1B expression in myeloma. *Leukemia* **20**, 2034–2040.

[11] Fonseca R, Blood E, and Rue M, et al (2003). Clinical and biologic implications of recurrent genomic aberrations in myeloma. *Blood* **101**, 4569–4575.

[12] Keats JJ, Reiman T, and Maxwell CA, et al (2003). In multiple myeloma, t(4;14)(p16;q32) is an adverse prognostic factor irrespective of FGFR3 expression. *Blood* **101**, 1520–1529.

[13] Davies FE, Dring AM, and Li C, et al (2003). Insights into the multistep transformation of MGUS to myeloma using microarray expression analysis. *Blood* **102**, 4504–4511.

[14] Lopez-Corral L, Gutierrez NC, and Vidriales MB, et al (2011). The progression from MGUS to smoldering myeloma and eventually to multiple myeloma involves a clonal expansion of genetically abnormal plasma cells. *Clin Cancer Res* **17**, 1692–1700.

[15] Walker BA, Wardell CP, and Chiecchio L, et al (2011). Aberrant global methylation patterns affect the molecular pathogenesis and prognosis of multiple myeloma. *Blood* **117**, 553–562.

[16] Radl J, Croese JW, Zurcher C, Van den Enden-Vieveen MH, and de Leeuw AM (1988). Animal model of human disease. Multiple myeloma. *Am J Pathol* **132**, 593–597.

[17] Radl J, De Glopper ED, Schuit HR, and Zurcher C (1979). Idiopathic paraproteinemia. II. Transplantation of the paraprotein-producing clone from old to young C57BL/KaLwRij mice. *J Immunol* **122**, 609–613.

[18] Claudio JO, Zhu YX, and Benn SJ, et al (2001). HACS1 encodes a novel SH3-SAM adaptor protein differentially expressed in normal and malignant hematopoietic cells. *Oncogene* **20**, 5373–5377.

[19] Wang D, Stewart AK, and Zhuang L, et al (2010). Enhanced adaptive immunity in mice lacking the immunoinhibitory adaptor Hacs1. *FASEB J* **24**, 947–956.

[20] Zhu YX, Benn S, and Li ZH, et al (2004). The SH3-SAM adaptor HACS1 is up-regulated in B cell activation signaling cascades. *J Exp Med* **200**, 737–747.

[21] Yamada H, Yanagisawa K, and Tokumaru S, et al (2008). Detailed characterization of a homozygously deleted region corresponding to a candidate tumor suppressor locus at 21q11-21 in human lung cancer. *Genes Chromosomes Cancer* **47**, 810–818.

[22] Davey RA, Hahn CN, May BK, and Morris HA (2000). Osteoblast gene expression in rat long bones: effects of ovariectomy and dihydrotestosterone on mRNA levels. *Calcif Tissue Int* **67**, 75–79.

[23] Livak KJ and Schmittgen TD (2001). Analysis of relative gene expression data using real-time quantitative PCR and the 2(-Delta Delta C(T)) Method. *Methods* **25**, 402–408.

[24] Diamond P, Labrinidis A, and Martin SK, et al (2009). Targeted disruption of the CXCL12/CXCR4 axis inhibits osteolysis in a murine model of myeloma-associated bone loss. *J Bone Miner Res* **24**, 1150–1161.

[25] Rayner JR and Gonda TJ (1994). A simple and efficient procedure for generating stable expression libraries by cDNA cloning in a retroviral vector. *Mol Cell Biol* **14**, 880–887.

[26] Isenmann S, Arthur A, and Zannettino AC, et al (2009). TWIST family of basic helix-loop-helix transcription factors mediate human mesenchymal stem cell growth and commitment. *Stem Cells* **27**, 2457–2468.

[27] Chesi M, Robbiani DF, and Sebag M, et al (2008). AID-dependent activation of a MYC transgene induces multiple myeloma in a conditional mouse model of post-germinal center malignancies. *Cancer Cell* **13**, 167–180.

[28] Radl J, Hollander CF, van den Berg P, and de Glopper E (1978). Idiopathic paraproteinaemia. I. Studies in an animal model–the ageing C57BL/KaLwRij mouse. *Clin Exp Immunol* **33**, 395–402.

[29] Fowler JA, Mundy GR, Lwin ST, Lynch CC, and Edwards CM (2009). A murine model of myeloma that allows genetic manipulation of the host microenvironment. *Dis Model Mech* **2**, 604–611.

[30] Garrett IR, Dallas S, Radl J, and Mundy GR (1997). A murine model of human myeloma bone disease. *Bone* **20**, 515–520.

[31] Oyajobi BO, Munoz S, and Kakonen R, et al (2007). Detection of myeloma in skeleton of mice by whole-body optical fluorescence imaging. *Mol Cancer Ther* **6**, 1701–1708.

[32] Vanderkerken K, De Raeve H, and Goes E, et al (1997). Organ involvement and phenotypic adhesion profile of 5T2 and 5T33 myeloma cells in the C57BL/KaLwRij mouse. *Br J Cancer* **76**, 451–460.

[33] Fowler JA, Lwin ST, and Drake MT, et al (2011). Host-derived adiponectin is tumor-suppressive and a novel therapeutic target for multiple myeloma and the associated bone disease. *Blood* **118**, 5872–5882.

[34] Noll JE, Williams SA, and Tong CM, et al (2013). Myeloma plasma cells alter the bone marrow microenvironment by stimulating the proliferation of mesenchymal stromal cells. *Haematologica* **99**, 163–171.

[35] Heller G, Schmidt WM, and Ziegler B, et al (2008). Genome-wide transcriptional response to 5-aza-2'-deoxycytidine and trichostatin a in multiple myeloma cells. *Cancer Res* **68**, 44–54.

[36] Cashman J, Eaves AC, and Eaves CJ (1985). Regulated proliferation of primitive hematopoietic progenitor cells in long-term human marrow cultures. *Blood* **66**, 1002–1005.

[37] Hurley RW, McCarthy JB, and Verfaillie CM (1995). Direct adhesion to bone marrow stroma via fibronectin receptors inhibits hematopoietic progenitor proliferation. *J Clin Invest* **96**, 511–519.

[38] Lwin T, Hazlehurst LA, and Dessureault S, et al (2007). Cell adhesion induces p27Kip1-associated cell-cycle arrest through down-regulation of the SCFSkp2 ubiquitin ligase pathway in mantle-cell and other non-Hodgkin B-cell lymphomas. *Blood* **110**, 1631–1638.

[39] Mitelman F, Mertens F, and Johansson B (1997). A breakpoint map of recurrent chromosomal rearrangements in human neoplasia. *Nat Genet* **15**, 417–474 [Spec No].

[40] Ni IB, Ching NC, Meng CK, and Zakaria Z (2012). Translocation t(11;14)(q13;q32) and genomic imbalances in multi-ethnic multiple myeloma patients: a Malaysian study. *Hematol Rep* **4**, 60–65.

[41] Kassambara A, Hose D, and Moreaux J, et al (2012). Genes with a spike expression are clustered in chromosome (sub)bands and spike (sub)bands have a

powerful prognostic value in patients with multiple myeloma. *Haematologica* **97**, 622–630.

[42] Bollati V, Fabris S, and Pegoraro V, et al (2009). Differential repetitive DNA methylation in multiple myeloma molecular subgroups. *Carcinogenesis* **30**, 1330–1335.

[43] Heuck CJ, Mehta J, and Bhagat T, et al (2013). Myeloma is characterized by stage-specific alterations in DNA methylation that occur early during myelomagenesis. *J Immunol* **190**, 2966–2975.

[44] von Holleben M, Gohla A, Janssen KP, Iritani BM, and Beer-Hammer S (2011). Immunoinhibitory adapter protein Src homology domain 3 lymphocyte protein 2 (SLy2) regulates actin dynamics and B cell spreading. *J Biol Chem* **286**, 13489–13501.

[45] Levesque JP, Zannettino AC, and Pudney M, et al (1999). PSGL-1-mediated adhesion of human hematopoietic progenitors to P-selectin results in suppression of hematopoiesis. *Immunity* **11**, 369–378.

[46] Kim CA and Bowie JU (2003). SAM domains: uniform structure, diversity of function. *Trends Biochem Sci* **28**, 625–628.

[47] Zarrinpar A, Bhattacharyya RP, and Lim WA (2003). The structure and function of proline recognition domains. *Sci STKE* **re8**, 1–10.